FINAL RESULTS OF THE NASA STORM HAZARDS PROGRAM

Bruce D. Fisher
NASA Langley Research Center
Hampton, VA 23665

Philip W. Brown
NASA Langley Research Center
Hampton, VA 23665

J. Anderson Plumer
Lightning Technologies, Inc.
Pittsfield, MA 01201

Lt. Col. Alfred J. Wunschel, Jr.
Air Force Systems Command
NASA Langley Research Center
Hampton, VA 23665

Presented at the International Conference on
Lightning and Static Electricity
April 19-21, 1988
Oklahoma City, Oklahoma

FINAL RESULTS OF THE NASA STORM HAZARDS PROGRAM

Bruce D. Fisher and Philip W. Brown
NASA Langley Research Center
Hampton, Virginia 23665
U.S.A.

J. Anderson Plumer
Lightning Technologies, Inc.
Pittsfield, Massachusetts 01201
U.S.A.

Lt. Col. Alfred J. Wunschel, Jr.
Air Force Systems Command
NASA Langley Research Center
Hampton, Virginia 23665
U.S.A.

ABSTRACT

Lightning swept-flash attachment patterns and the associated flight conditions were recorded from 1980-1986 during 1496 thunderstorm penetrations and 714 direct strikes with a NASA F-106B research airplane. These data were studied with an emphasis on lightning avoidance by aircraft and on aircraft protection design. The individual lightning attachment spots, along with crew comments and on-board photographic data were used to identify lightning swept-flash attachment patterns and the orientations of the lightning channels with respect to the airplane. During the 1986 season, the airborne photographic system included two video cameras which were installed on the top of the left wing tip with overlapping fields of view encompassing the side of the airplane from the nose boom to the trailing upper apex of the vertical tail. These cameras provided unique in-flight documentation of the lightning swept-stroke phenomenon. The full-scale in-flight data were compared to results from scale-model arc-attachment tests. The airborne and scale-model data showed that any exterior surface of this airplane may be susceptible to direct lightning attachment. In addition, the altitudes, ambient temperatures, and the relative turbulence and precipitation levels at which the strikes occurred in thunderstorms are summarized and discussed. It was found that the peak strike rate occurred at pressure altitudes between 38 000 ft and 40 000 ft, corresponding to ambient temperatures colder than -40°C.

1. INTRODUCTION

Many new aircraft designs will include the use of composite materials for primary aircraft structure and skins, and digital avionics for flight and engine controls and systems management. Although these new technologies promise improvements in aircraft performance and efficiency, their use will require that more specific lightning protection methods be incorporated in the design of new airframes and systems in order to maintain the excellent lightning safety record presently enjoyed by transport aircraft [1 and 2]. This excellent safety record can be attributed to the widespread use of aluminum (an excellent electrical conductor) as a skin and structural material, and the use of mechanical and hydraulic control systems, which are relatively immune to the adverse effects of lightning. However, even in aircraft designs utilizing proven design techniques, a few lightning catastrophies have occurred [3-5]. Therefore, complacency in the design of aircraft lightning protection and in aircraft operations is not warranted.

Significant insights into these lightning-related issues were made during the NASA Langley Research Center Storm Hazards Program, which was conducted to improve the state of the art of severe storm hazards detection and avoidance, as well as protection of aircraft against those hazards which cannot reasonably be avoided. Following a preliminary phase in which a commercially-available airborne lightning locator was flown on the periphery of thunderstorms [6 and 7], a specially-instrumented and lightning-hardened NASA F-106B airplane was flown through thunderstorms to elicit in-flight lightning strikes. The data from these thunderstorm penetrations were used to quantify the electromagnetic characteristics of in-flight lightning strikes, to identify atmospheric conditions conducive to such strikes, to clarify some of the more questionable aspects of establishing lightning strike zones on the exterior of aircraft, and to study leader initiation/vehicle triggering of lightning strikes.

During the 1980-1986 thunderstorm seasons, the F-106B airplane made 1496 thunderstorm penetrations during which 714 direct lightning strikes were experienced. These flights were made in Oklahoma and Virginia in conjunction with ground-based guidance and measurements by the NOAA National Severe Storms Laboratory (NSSL) and the NASA Wallops Flight Facility, respectively. Starting in 1982, the UHF-band radar at NASA Wallops was used to direct the F-106B airplane to electrically-active regions of the thunderstorms and to provide instrumental data used to determine if the lightning strikes were random encounters with naturally-occurring lightning channels or if the strikes were triggered by the airplane itself [8 and 9].

The purposes of this paper are: to summarize those thunderstorm conditions found in this program to be conducive to aircraft lightning strikes; to discuss the lightning-strike attachment zones found on the F-106B airplane; to provic an example of the capabilities of the airborne photographic systems; and, to briefly summarize the results of the other experiments conducted during this program. The data in this paper update that previously presented to this forum [10-12].

2. DESCRIPTION OF THE EXPERIMENT

2.1 F-106B Research Airplane

A thoroughly-instrumented and lightning-hardened NASA F-106B "Delta Dart" airplane (Fig. 1) was used to make thunderstorm penetrations starting in 1980 [10-

12]. The principal lightning hardening procedures [7 and 13] consisted of removing paint from most exterior surfaces of the airplane; installation of surge protective devices and electromagnetic shielding of electrical power and avionic systems; and, using JP-5 (or Jet A) fuel in lieu of the JP-4 (Jet B) fuel used in the U.S. Air Force F-106 fleet. Prior to each thunderstorm season, the lightning-hardening integrity was verified during ground tests in which simulated lightning currents and voltages of greater than average intensity were conducted through the airplane with the airplane manned and all systems operating [13].

The airplane altitude, Mach number, attitudes, ambient temperature, position, and other flight conditions were measured by the Aircraft Instrumentation System (AIS) and the Inertial Navigation System (INS) [10 and 14]. The direct-strike lightning instrumentation system [15-18] recorded electromagnetic waveforms from direct lightning strikes and nearby lightning flashes in flight using electromagnetic sensors located throughout the airplane and a shielded recording system located in the internal weapons bay.

The lightning attachments to the exterior of the airplane were filmed by combinations of eleven onboard cameras [10, 19, 20, and 21]. In 1986, only eight cameras were used; the locations and fields of view of these eight cameras are shown in Figure 2 and their characteristics are summarized in Table 1. These cameras were:

- one 16-mm movie camera mounted under a fairing on the left side of the fuselage, looking aft with a field of view including the left wing tip and vertical tail
- one black and white video camera installed in the cockpit between the pilot's ejection seat and the flight test engineer's forward instrument panel, facing aft with a field of view encompassing both wing tips
- one black and white video camera installed in the cockpit between the pilot's ejection seat and the flight test engineer's forward instrument panel, facing forward with a field of view centered on the nose boom
- one black and white video camera installed in the air conditioner access compartment aft of the cockpit, facing upward with a 60° field of view (removed following installation of the wing tip video pod described below)
- two black and white video cameras installed in a pod mounted on the upper surface of the left wing tip with overlapping fields of view encompassing the airplane from just ahead of the nose boom to the trailing upper apex of the vertical fin cap (Fig. 3)
- three 70-mm still cameras installed on the same platform as the cockpit video cameras, with two cameras facing forward to provide a stereo pair, and one camera facing aft with the same field of view as the cockpit-mounted aft-facing video camera.

In addition, the airplane was equipped with a commercially-available X-band color digital weather radar [7] and a commercially-available airborne lightning locator system [6 and 7].

2.2 Ground-Based Support

For the research flights made in Oklahoma in 1980 and 1981, the NOAA-NSSL Doppler radar at Norman, OK was used to measure the precipitation reflectivity and wind velocity data [14]. In addition, an incoherent 10-cm wavelength surveillance radar was used to provide air traffic control guidance to the airplane.

During storm penetrations in Virginia, the UHF-band (70.5-cm wavelength) and S-band (10-cm wavelength) radars at the NASA Goddard Space Flight Center/Wallops Flight Facility were used to locate lightning flashes and to determine precipitation reflectivity, respectively. The radar specifications are described by Mazur, et al. [8], and the ground-based systems used at NASA Wallops in support of the Storm Hazards Program are described by Gerlach and Carr [22].

For those missions which occurred in Virginia, the primary responsibility to launch and recall the airplane, select the storms and altitudes of interest, and provide real-time flight support and guidance to the aircrew was assigned to the Storm Hazards project personnel located in a dedicated area of the NASA Langley flight service station. The NASA Langley personnel worked in concert with their counterparts at NASA Wallops, with real-time discussions of radar data and flight strategy taking place over a dedicated telephone line between the two sites. Personnel at both sites could communicate with the flight crew via radio. Generally, the airplane was flown within 150 n.mi. of NASA Langley to maintain line of sight communications with NASA Langley and NASA Wallops. The systems and displays used are described by Fisher, Brown and Plumer [19] and Fisher, et al. [23].

In addition to the ground-based guidance from NASA Langley and NASA Wallops, the pilots also used data from an onboard X-band digital weather radar to avoid areas of 50 dBZ, or greater, precipitation reflectivity, and other areas where hail might be encountered. The thunderstorm penetration procedures which were used are described by Fisher and Plumer [7].

3. DISCUSSION OF RESULTS

3.1 Flight Conditions Conducive to Aircraft Lightning Strikes

The number of missions, thunderstorm penetrations, direct strikes and nearby flashes (lightning channels close enough to the airplane to trigger the onboard lightning instrumentation without actually attaching to the airplane) for the Storm Hazards 1980-1986 seasons are summarized by year in Table 2. The data show that the 184 thunderstorm research missions resulted in 714 direct lightning strikes and 188 nearby flashes during 1496 penetrations. The geographical location of the F-106B airplane at the time of each direct strike and nearby flash is shown in Figures 4(a) and 4(b).

Histograms showing the number and durations of penetrations, and the number of strikes and nearby flashes experienced from 1980-1986 are shown for altitude intervals of 2000 ft in Figure 5, and for ambient temperature intervals of 5°C in Figure 6. Penetrations were made by the F-106B airplane at pressure altitudes ranging from 2400 ft to 40 000 ft with a mean penetration altitude of 22 900 ft (Fig. 5). Temperature data (mean value during the penetra- tion) were available for 1368 penetrations, with values ranging from 20°C to -60°C, with an overall mean value of -19°C (Fig. 6). The distributions of penetration duration time with altitude and ambient temperature are very similar to the corresponding penetration distributions.

A plot of lightning strike incidents as a function of altitude for commercial aircraft in routine operations is shown in Figure 7 (from [2] with updated data from [1]). Based on data such as that shown in Figure 7, most penetrations in the 1980 and 1981 seasons were made at altitudes corresponding to ambient temperatures between ±10°C in expectation of receiving a large number of strikes. However, very few strikes were experienced (see Table 2). Starting in 1982, the NASA Wallops UHF-band radar was used to guide the F-106B airplane through the upper electrically-active regions of thunderstorms [8 and 24], resulting in hundreds of high altitude direct lightning strikes (Table 2 and [8, 10, and 20]). Starting in the 1984 season, the UHF-band radar was used to provide guidance to electrically-active regions in thunderstorms at altitudes below 20 000 ft [9], the same range of altitudes studied previously in 1980 and 1981. The low altitude research efforts of 1980-81 and 1984-86 are shown in the low altitude/warm temperature peaks in the penetration and duration data in Figures 5 and 6.

The Storm Hazards Program strike statistics shown in Figures 5 and 6 differ significantly from the published strike data for commercial aircraft ([1 and 2] - see Fig. 7) and for U.S. Air Force aircraft [3], in which most lightning strikes were found to occur between ambient temperatures of ±10°C. In the Storm Hazards Program, direct strikes were experienced at pressure altitudes ranging from 14 000 ft to 40 000 ft with a mean value of 20 600 ft (Fig. 5). The corresponding ambient temperature values ranged from 5°C to -65°C, with a mean value of -30°C (Fig. 6). The nearby flash data are very similar to the direct strike data.

Despite spending approximately 1559 mins of penetration duration time at altitudes below 20 000 ft (37 percent), only 98 direct strikes were experienced (14 percent) (see Table 2). In fact, the peak strike rates in Figure 5 of 7 strikes/penetration and 1.4 strikes/min occurred at pressure altitudes between 38 000 ft and 40 000 ft corresponding to ambient temperatures colder than -40°C. (During one research flight through a thunderstorm anvil at 38 000 ft altitude in 1984, the F-106B airplane experienced 72 direct strikes in 45 mins of penetration time, with the instantaneous strike rate twice reaching a value of 9 strikes/min.) On the other hand, the peak strike rate near the freezing level (0°C) was only 0.1 strike/min (in the altitude interval between 18 000 ft and 20 000 ft, corresponding to ambient temperatures of -5°C to -10°C).

The NASA Storm Hazards pressure and temperature lightning strike statistics differ from the commercial and U.S. Air Force data for two reasons. First, the NASA data came solely from intentional thunderstorm penetrations, while the commercial and military data were derived from a variety of meteorological conditions, mostly in non-thunderstorm clouds. For example, some of the commercial airline strikes were reported in snow storms or in winter time nimbostratus clouds [1]. U.S. Air Force aircraft have reported lightning strikes in cirrus clouds downwind of previous thunderstorm activity, in cumulus clouds around the periphery of thunderstorms, and even in stratiform clouds and light rain showers not associated with thunderstorms [25]. (The NASA Storm Hazards Program did not study the non-thunderstorm lightning strike phenomenon.) Second, commercial and military aircraft will normally deviate from course to avoid thunderstorms which reach cruise altitudes, and only penetrate when required to do so in the terminal area, where typical assigned altitudes are near the freezing level. Therefore, the NASA distributions of lightning strikes with respect to pressure altitude and ambient temperature differ from the commercial/military data because of the higher percentage of time spent by the NASA F-106B research airplane in the upper flash density center of thunderstorms, compared with the low percentage of time spent in thunderstorms at those altitudes by aircraft in routine operations. However, lightning strikes have been encountered at nearly all temperatures and altitudes in the Storm Hazards Program, indicating that there is no altitude at which aircraft are immune from the possibility of a lightning strike in a thunderstorm.

Although these Storm Hazards data differ from the commercial/military data, there is strong agreement with the results of two other thunderstorm flight test programs. The high altitude strike data are in good agreement with the results of the U.S. Air Force Rough Rider Program [26], in which the peak lightning activity was found to occur at an ambient temperature of -40°C. In addition, the low altitude strike data are nearly identical to the data from the USAF/FAA Convair 580 low altitude lightning measurement program [27], in which 63 percent of the 21 strikes experienced by that airplane occurred at an altitude of 18 000 ft, although only 16 percent of the flying time was spent at that altitude.

The most successful piloting technique used in searching for lightning was to fly through the thunderstorm cells which were the best defined visually and on the airborne weather radar. Frequently, heavy turbulence and precipitation were encountered during these penetrations. However, the lightning strikes rarely occurred in the heaviest turbulence and precipitation, and occasionally, there was no lightning activity whatsoever. These findings are shown in Figure 8, in which the percentage of direct strikes to the F-106B airplane is plotted as a function of the flight crew's opinion of relative turbulence and precipitation intensity at the time of the strikes. The data are plotted for those strikes which occurred above and below 20 000 ft altitude. In both altitude regimes, most lightning strikes (approximately 80 percent) occurred in thunderstorm regions in which the crews characterized the turbulence and precipitation as negligible to light. In addition, although a strong correlation between lightning strikes and vertical drafts (predominantly downdrafts) was found for a small data set in 1981 and 1982, most strong turbulence episodes encountered by the airplane were not associated with lightning [28 and 29].

Unlike the temperature and altitude data discussed above, there is no discrepancy between the precipitation and turbulence data gathered in this program and that data gathered during commercial [1 and 2] and military operations [3]. As before, the data are in agreement with those from the USAF/FAA Convair 580 program [27]. Commercial aircraft reported that 77 percent of all strikes occurred in light to moderate turbulence, with 22 percent of all strikes occurring with no turbulence. Eighty-one percent of all commercial strikes occurred in rain; only 2 percent of the strikes were associated with rain and hail. For military aircraft, only 20 percent of the strikes were associated with turbulence, 67 percent of the strikes occurred in rain, 5 percent occurred in hail or snow, and 10 percent occurred in "clear air." Finally, for the Convair 580 research program, 90 percent of the strikes occurred in light to negligible turbulence; all the strikes were associated with rain. In summary, the thunderstorm research data gathered by the NASA F-106B airplane and the USAF/FAA Convair 580 airplane, as well as the commercial/military data, have shown that the number of direct strikes to aircraft do not show a positive correlation to turbulence and precipitation intensities.

Although the Doppler radar data recorded in 1981 and 1982 using the NASA Wallops S-band radar [28] showed heavy turbulence within the high precipitation reflectivity cores of thunderstorms, heavy turbulence also was found between cells, near storm boundaries, and in innocuous-appearing low reflectivity factor regions. Similar results were found during the multi-year Rough Rider Program turbulence studies [30]. Therefore, it can be concluded that turbulence and precipitation also are not necessarily correlated.

3.2 Airborne Photography

Removal of most paint from the exterior metal surfaces of the airplane in order to minimize the lightning dwell times [7] made it very difficult to track the swept-stroke attachment paths because of the small size of the melted spots. Therefore, the onboard camera systems provided the primary means of documenting these patterns. One example of the photographic coverage possible with the system used in 1986 is provided by the photographs from strike 23 of 1986. Coverage was provided by the four video cameras in use (fore- and aft-viewing cameras in the cockpit and the two cameras on the left wing tip). The photoelectric diodes in the cockpit also sensed the strike, actuating the 16-mm movie camera and the three cockpit-mounted 70-mm still cameras.

For strike 23 of 1986, the onboard camera systems were used to confirm that a lightning strike had occurred to the nose boom, and that this strike was probably a random intercept of a naturally-occurring lightning channel. At the time of the strike, the flight test engineer, sitting in the rear seat, asked the research pilot if they had taken "another hit." The pilot replied that he did not see the channel attach, but that he saw many channels "right in front of the airplane." Also at this time, the two tape recorders in the direct strike lightning instrumentation system stopped running, although the other data and flight systems were unaffected.

It is known that the channel attached to the nose boom from the photographs taken by the two forward-facing still cameras. An extremely tortuous lightning channel can be seen attached to the right side of the nose boom in the photograph taken by the camera mounted on the right side of the cockpit (Fig. 9). The left-side view (not shown) was similar, with the exception that large portions of the channel were blocked from view by the canopy structure.

This same channel and structure also can be seen in three successive frames from the cockpit-mounted, forward-facing video camera (Fig. 10). Figure 10(a) shows a reference shot from this camera in daylight on the runway; the airborne frames are shown in Figures 10(b-d). The lightning channel appears to be ahead and above the nose boom at 20:23:27.333 UT (Fig. 10(b)); in the next frame, at 20:23:27.367 UT (Fig. 10(c)), the channel appears closer to the aircraft, to the right of the forward fuselage. Finally, in the third frame, at 20:23:27.434 UT (Fig. 10(d)), the channel is attached to the nose boom, with the same characteristic loop and tortuousity as shown with more clarity in the still photographs (Fig. 9).

The corresponding views from the forward-facing camera on the left wingtip are shown in Figure 11. Similarly to Figure 10, the data frames (Figs. 11(b-d)) are preceded by a reference frame taken in daylight (Fig. 11(a)). From the wing-tip vantage point, it is not possible to determine conclusively if the lightning channel actually attaches to the nose boom. However, it appears that the channel is attached at 20:23:37.44 UT (Fig. 11(d)). No lightning channels are visible in the fields of view of either forward-facing video camera following this time. The similarity in the tortuousity and geometry of the lightning channel shown in Figures 9-11 provides assurance that the same channel is being observed.

No confirmed lightning attachments could be discerned in the views from the four aft-facing cameras. The aft-facing, cockpit-mounted video camera frames (not shown in the paper) show the reflected image of a lightning channel on the right side of the flight test engineer's helmet visor at 20:23:27.438 UT (corresponding in time to the views shown in Figs. 10(d) and 11(d)), followed by five successive frames in which a dimly-lit lightning channel was seen in the aft rear quadrant of the airplane, behind the right wing. The photograph from the aft-facing still camera (also not shown because of poor contrast) contains the same lightning image. The empennage-facing, wing-tip-mounted video camera frames do not contain images of lightning channels, but do show a brightening of the underside of the fuselage near the afterburner for four consecutive frames from 20:23:27.321-27.456 UT.

The final photographic data analyzed were from the fuselage-mounted, aft-facing 16-mm movie camera. Following actuation by the cockpit-mounted, light-sensing diodes, the camera exposed 167 frames of film at a nominal frame rate of 200 frames/sec, with lightning activity evident in the first 62 frames of the sequence. In the second frame (the first frame was overexposed) a detached channel was seen behind the left wing of the airplane (not shown in this paper because of poor contrast). This channel apparently was too dim to be seen by the aft-facing video camera in the cockpit. In fact, this channel may be a different channel from that which attached to the nose boom. In the third frame of this sequence, Figure 12, a lightning channel can be seen behind the engine and tail, with no apparent attachment to the airplane. The portion of the channel which is blocked from view by the vertical tail is believed to be the channel which appears behind the right wing in the fields of view of the aft-facing video and still cameras mounted in the cockpit.

In summary, the photographic data associated with strike 23 of 1986 strongly suggest that this strike was a random intercept of a naturally-occurring channel, with momentary contact occurring to the nose boom. Following contact, the channel either swept aft a short distance under the fuselage, or the airplane flew out of the channel, with the airplane passing over the top of the channel. Although research in this program has shown that most of the strikes to the F-106B airplane were triggered by the airplane [8, 9, 31, and 32], intercepted flashes also have been detected [9], especially at the lower altitudes in thunderstorms. (At the time of this strike, the F-106B airplane was at an altitude of 15 000 ft and an ambient temperature of -2°C.)

As was the case with most strikes to the F-106B airplane, subsequent pulses in luminousity were detected. The cockpit-mounted, aft-facing video camera, with a time resolution of 33 msec, showed three subsequent pulses. The movie camera, with a time resolution of approximately 5 msec showed four subsequent pulses. These pulses in luminousity have been ascribed by Mazur [32] to current surges associated with negative stepped leaders, recoil streamers and return strokes.

3.3 Lightning Attachment Patterns

Photographic data, such as shown in this paper, have been used to document the swept-flash attachment patterns on the exterior of this airplane. In addition, these data have been used, in conjunction with the airborne electromagnetic waveform data and ground-based radar measurements of lightning echo location, to analyze lightning initiation on aircraft in thunderstorms [8, 9, 31, and 32]. A summary of those strikes which have been studied in detail for these purposes is given in Table 3. The NASA effort in the clarification of lightning strike zones will be discussed in the remainder of this section.

The full-scale in-flight data have shown that there were four general strike scenarios in the swept flash attachment patterns on the exterior of this airplane [7 and 12]:

1. Flashes which initially attach to the nose of the aircraft and subsequently "sweep" alongside it, reattaching at a succession of spots along the fuselage. In these cases, the initial and final exit point is usually the trailing edge of an extremity such as a wing or vertical fin tip. The final entry point is a trailing edge of the fuselage, because the flash is usually still alive by the time the aircraft has flown completely through it.
2. Similar to (1) except that the entry channel sweeps aft across the top or bottom wing surface instead of the fuselage.
3. Strikes in which the initial entry and exit points occur at the nose. In this case, the lightning flash appears to "touch" the aircraft nose but continues on from this point to another destination. The aircraft then flies through the flash, resulting in successive entry points along one side of the fuselage or wing and exit points along the other. Again, because the flash usually exists for a longer time than it takes the aircraft to fly its length, the final entry and exit points are located along trailing edges.
4. Strikes in which the initial and final entry and exit points are confined to the aft extremities.

With most of these general scenarios, swept-flash channels frequently have been found which rejoin behind the airplane after the airplane has flown through the channel. These same four attachment patterns also have been identified on the FAA/USAF Convair 580 airplane [27].

Lightning strike zones on aircraft have been defined as follows [33]:

- Zone 1A - Initial attachment point with low possibility of lightning arc channel hang-on. Surfaces within this zone include the aircraft nose, engine nacelles, and the forward surfaces of wing tips. Zone 1A includes those areas in which the first return stroke of a cloud-to-earth lightning flash will attach.
- Zone 1B - Initial attachment point with high possibility of lightning arc channel hang-on, such as the trailing edges of extremities. All lightning flash currents are expected to enter/exit in this zone.
- Zone 2A - A swept-stroke zone with low possibility of lightning arc channel hang-on, such as fuselage surfaces aft of Zone 1A. Only a subsequent stroke (re-strike) and some continuing currents of low amplitude are expected to occur in this zone.
- Zone 2B - A swept-stroke zone with high possibility of lightning arc channel hang-on. This zone includes surfaces aft of Zone 2A, such as the trailing edges of some flight control surfaces.
- Zone 3 - All of the vehicle areas other than those covered by Zone 1 and 2 regions. In Zone 3, there is a low possibility of any attachment of the lightning channel; however, structures in this zone usually must conduct Zone 1A or 1B currents since they usually lie between some pair of attachment points. These currents may affect systems or components located within the aircraft.

The intensities of lightning currents expected in each of the zones described above have been defined for design and certification purposes [33-35]. In general, surfaces and structures located in Zones 1A and 1B receive more intense currents, and therefore, may have to be provided with greater degrees of protection than surfaces in other zones.

Although there are guidelines for determining the location of each zone on specific airplanes [33 and 34], such was not done for the F-106 airplane since it was designed prior to the creation of the specifications. Application of the zones to an existing aircraft can be controversial, due to differing interpretations of the guidelines. However, in the case of the Storm Hazards Program's F-106B airplane, it was possible to locate the zones on the airplane's exterior from direct observation of the lightning attachment patterns left from the 714 direct lightning strikes which were experienced.

Applying the zone definitions to the four attachment patterns discussed earlier resulted in the F-106 lightning attachment zones shown in Figure 13. These swept-flash attachment zones have been described previously [7 and 12]. The principal features may be summarized as follows:

- the Zone 1A region includes those surfaces up to 180 in. aft of the tip of the nose boom
- the upper portion of the canopy also is considered Zone 1A because it represents a significant projection above the fuselage. It is thought that some leaders have initially struck or originated from the canopy of the NASA F-106B airplane.
- the Zone 1B region includes the afterburner, including the area up to 14 in. inside the afterburner
- there are no Zone 3 surfaces on this airplane; i.e., the entire exterior surface of this airplane is susceptible to "direct" or "swept" lightning strike attachments. The underlying structures throughout the aircraft are within Zone 3, however, since the structures must conduct lightning currents between various pairs of lightning entry and exit points.

The extension of Zone 1A 180 in. aft of the tips of the forward initial leader attachment points (the nose boom and the canopy brow) accounts for the distance the aircraft travels prior to arrival of the first return stroke. The Zone 1A environment is based on a severe cloud-to-earth flash containing a first return stroke of 200 kA [33 and 34]. Operational data have shown that most strokes of this magnitude are experienced by aircraft flying at altitudes below 4500 m (15 000 ft). If a leader is assumed to propagate at an average velocity of 1.5×10^5 m/sec, and the F-106B airplane is assumed to fly at approximately 300 knots (150 m/sec) at these altitudes, the distance, d, travelled by the airplane following an initial leader attachment to the airplane is approximately [35]:

$$d = \frac{(4500m)\ (150\ m/sec)}{(1.5 \times 10^5\ m/sec)} = 4.5\ m \text{ or } 177 \text{ inches}$$

Thus, a Zone 1A extension of 180 inches has been assumed for the F-106B airplane, as shown in Figure 13.

The possibility of leaders sweeping a significant distance aft of initial attachment points prior to first return stroke occurrence has not been widely recognized until recently. Formerly, it was assumed that first return stroke occurrence was synonymous with leader attachment, and that Zone 1 was limited to surfaces within 18 inches (or so) of leading-edge extremities. On a conventional aluminum aircraft, the precise extension of Zone 1A makes little practical difference. However, the Zone 1A environment (200 kA, $2 \times 10^6\ A^2$ sec [33, 34, and 36]) is much more damaging to composite skins and structures than the Zone 2A environment (100 kA, $0.25 \times 10^6\ A^2$ sec). Therefore, the possibility of severe first return stroke arrival a significant distance aft of leading edges must be accounted for by appropriate extensions of Zone 1A.

To further clarify the locations of the possible initial leader attachment areas on the full-scale F-106B airplane, scale-model lightning attachment point tests have been conducted using test techniques established by the Society of Automotive Engineers [36]. In these tests, a 10-percent scale model of the F-106B airplane, which had been painted with a conductive coating, was mounted on a dielectric stand which allowed the three aircraft attitude angles (pitch, roll, and yaw) to be adjusted. The model was positioned approximately midway between a rod electrode suspended above the model and a ground plane beneath the model. The rod electrode was used to represent the tip of a lightning leader advancing toward the aircraft, and the ground plane represented a diffuse region of opposite polarity charge.

The simulated lightning leaders were discharged from the high voltage electrode which was connected to the output of a 1.5 MV Marx-type generator. The air gap distance from the electrode to the surface of the model was approximately 4 feet with an additional gap of approximately 3 feet formed between the model and the ground plane. The gap distances were arbitrarily chosen within constraints of model size and facility dimensions. Ideally, larger air gaps would seem to be more representative of a naturally-occurring lightning leader approaching from a remote charge center. However, repositioning of the electrode further away from the model resulted in some strikes bypassing the model altogether.

A test voltage of approximately 25 μsec duration was applied between the electrode and the ground plane. The voltage time duration was set to 20-25 μsec in order to allow development of streamers and attachment points in regions of lower field intensity (in addition to those of high intensity at surfaces of high strike probability).

When test voltage is applied between the electrode and the ground plane, an electric field exists across the air gaps between electrode and model and between the model and the ground plane. Ionization occurs initially at the rod electrode, in the form of streamers which propagate in the general direction of the model, in the manner of leaders approaching an aircraft. This intensifies the electric field about the model. When the field adjacent to the model surfaces reaches an ionizing level, streamers develop at the model and propagate into the field, towards the "leader" and towards the ground plane. Those streamers that intercept a "leader" from the electrode and the streamers from the ground plane establish the initial leader attachment points for the particular test. Once ionization of the air gap is complete, the electric fields diminish to a non-ionizing level and no additional streamers or attachment points develop. In order to identify all possible attachment points, it is necessary to position the model and electrode at a variety of orientations representing lightning leaders approaching the aircraft from different directions, and to apply repeated tests from each electrode position because streamer propagation paths vary from discharge to discharge, resulting in a statistical variation among resulting attachment points.

Each of the high-voltage discharges was recorded on photographic film by three 35-mm cameras. Two of these cameras were attached to tripods at the approximate height of the model and located approximately 60-90 degrees apart from each other. A third camera was positioned approximately 3 feet above the model to provide an overhead view of the strike attachments. Each camera was loaded with ASA 100 color print film and its lens aperture set at f/5.6. Lighting for the model was supplied by the high voltage arc and two electronic flash units. The lens apertures and the intensities of the electronic flash units were varied at times during the tests to achieve the best combination of background lighting and streamer photography.

The majority of the tests performed during this program were at positive electrode polarity with respect to the ground plane with a small number of tests performed at negative electrode polarity. Each model/electrode orientation was subjected to ten discharges of a given polarity.

Typical initial leader attachments to the scale model are shown in Figures 14-16. The scale-model tests showed initial attachment points to include the radome and nose boom (Fig. 14), canopy (Fig. 14), forward and center fuselage areas, wing tips (Fig. 15), engine inlet, engine exhaust nozzle (Fig. 16), and vertical fin (Fig. 15). In addition to wing-tip attachments, some leaders also attached to the wing leading edges (Fig. 16). In fact, on some tests multiple leader attachments between the rod electrode and the airplane were noted (Fig. 15).

Initial leader attachments to non-extremities such as the wing leading edges, engine inlets and top of the fuselage have not been expected to occur to such surfaces on vehicles with sharp extremities such as the nose boom and wing tips on the F-106 airplane [33], although this result confirms the suspected occurrence of leading edge and canopy strikes to the full-scale NASA F-106B research airplane. Even though initial attachments to the wing leading edge were seen in the model tests, the leading edge was left in Zone 2A, since it is felt that for such attachments to occur, the lightning channel must approach rather close to the aircraft prior to inducing streamers from the aircraft extremities. This small distance implies that the electric charge and corresponding electric field between the leader and the aircraft must be comparatively low, so that an ensuing return stroke would not have as high a rate of charge flow as that assigned to the first return stroke (current component A, 200 kA) associated with Zone 1A [33, 34]. This hypothesis is supported by the small size of the burn marks found on the leading edge of the wing following a strike in which initial attachment is believed to have occurred to that area.

The electrode arrangement utilized in these model tests is most representative of the aircraft intercepting a naturally-occurring lightning strike

[9]. To represent a "triggered" strike, in which streamer activity begins at the aircraft [32], the model probably should be immersed in a more uniform electric field, established by large parallel-plate electrodes. Nonetheless, the initial leader attachment locations resulting from the scale-model tests include all those which are believed to have occurred to the full-scale F-106B research airplane. The similarity in results from the two methods indicates that the electric fields in the immediate vicinity of the aircraft during each type of strike are similar, as postulated by Rudolph, et al. [37]. (The subsequent propagation of leaders away from the aircraft are, of course, different for the two types of strikes.) Finally, the similarities in the results demonstrate the usefulness of model tests in predicting initial lightning attachment points on aircraft.

In summary, the NASA Storm Hazards Program constituted the first systematic study of lightning attachment patterns on a full-scale aircraft in flight. The lightning attachment zones shown in Figure 13 imply that new aircraft designs using delta wings or highly-swept wing leading edges probably will require surface protection from lightning attachments over the complete exterior, an especially significant design feature for vehicles incorporating surfaces of composite materials. In addition, the lightning attachments within the tail pipe of the airplane have shown that engines and associated control and instrumentation systems may require lightning protection, especially if "fly-by-wire" controls are employed without mechanical backup.

3.4 Additional Experiments

Although this paper has concentrated on discussions of those conditions conducive to aircraft lightning strikes and of the lightning attachment patterns left on the exterior of the airplane, a number of other experiments were conducted during the Storm Hazards Program. In fact, the principal experiment was the quantification of aircraft-lightning electrodynamics, including airborne electromagnetic measurements and computer modeling. The results of the other Storm Hazards experiments are summarized briefly in this section.

- Electromagnetic measurements - The NASA F-106B airplane acquired considerable data on the rates of change of electromagnetic parameters on the aircraft surface. These in-situ measurements have provided the basis for the first statistical quantification of the lightning electromagnetic threat to aircraft appropriate for determining the indirect effects of intracloud flashes on aircraft. These results have been discussed by Lee, et al. [17] and Pitts, et al. [18]. Heretofore, the lightning threat for determining indirect effects has been based solely on cloud-to-earth lightning characteristics recorded by ground-based instruments.
- Lightning-aircraft interaction modeling - In order to understand the lightning data collected from the thunderstorm penetrations by the F-106B airplane, it was necessary to model the lightning-aircraft interaction. These models included both nonlinear models for analyzing the physics of a lightning event and linear models for analyzing the interaction in a simplified, or engineering, sense. Reasonable results were obtained between the models and the measured responses, providing increased confidence that the models may be credibly applied to other aircraft types and used in the prediction of internal coupling effects in the design of lightning protection of new aircraft. These models are described by Pitts, et al. [18].
- Aircraft-triggered lightning - The research conducted in the NASA Storm Hazards Program provided the first instrumental proof, using onboard camera systems and the ground-based UHF-band radar at NASA Wallops, of aircraft-triggered lightning flashes originating at the aircraft [8 and 9]. However, the UHF-band radar data also indicated that intercepted strikes can occur, with most intercepted strikes in thunderstorms occurring at altitudes below 20 000 ft [9]. Rudolph, et al. [37] have modeled the triggered-lightning phenomenon, including air-chemistry coefficients and the effects of aircraft size and shape. Their model has shown that a sharp-edged metal object on an aircraft will concentrate the local field sufficiently to trigger a local breakdown in the presence of an ambient electric field of proper magnitude and orientation, with the streamers propagating from the aircraft outward to charge centers. Perala and Rudolph [38] also have applied their model to an Atlas-Centaur expendable launch vehicle. Mazur [32] has developed a complementary physical model of the initiation of lightning flashes by aircraft using airborne photographic and electromagnetic data. Mazur believes that a triggered flash starts with either a negative corona or positive leader, depending on the ambient electric field vector and the airplane form factor. The positive leader, with continuous current which changes with time, is followed in a few milliseconds by the negative stepped leader with current pulses of a few kA magnitude. The two leaders develop in space simultaneously and bi-directionally from the oppositely-charged extremities of the airplane.
- Intracloud and cloud-to-ground strikes to aircraft - Mazur [32] has found that most strikes to the F-106B airplane were of the intracloud variety, and closely resembled natural intracloud flashes. However, it has been found that the airplane was involved in several cloud-to-ground flashes [9], including one flash which was triggered by the airplane with a return stroke current flow through the F-106B airplane [31]. However, the data set of confirmed cloud-to-ground strikes to the airplane was too small to arrive at a statistically sound conclusion regarding the cloud-to-ground strike threat.
- Atmospheric electrical modeling - In order to maximize the lightning strike rate to the F-106B airplane at low altitudes, Helsdon [39] used his two-dimensional storm electrification model to simulate the thunderstorm environment in which the airplane was flying. During this effort a lightning parameterization scheme was used for the first time within the context of a multidimensional cloud electrification model. Based on Helsdon's study and complementary radar studies by Mazur [9], an operational procedure was adopted for the 1986 field season. Even though the lightning parameterization scheme used was crude and the lack of understanding of how the lightning mechanism acts in a cloud is great, the model results were qualitatively consistent with the observations which were available.
- Electric field measurements - The effect of the location of electric field mills on the accuracy of electric field measurements with airplanes was evaluated using the F-106B airplane and its field mill locations as a test case [40]. It was shown that the sensors'

positions significantly affect the propagation of errors in estimates of aircraft enhancement factors and in signal processing. Mazur, et al. [40] felt that a technique utilizing small-scale modeling and computer-simulated block modeling of the airplane and sensor locations can produce an accuracy better than that attainable from in-flight calibrations alone.

- Comparison of airplane responses to natural lightning and simulated electromagnetic pulse (EMP) - Because of the very fast rise times measured for the lightning electromagnetic data [17 and 18], the Air Force Weapons Laboratory (AFWL) initiated a program to identify and quantify the similarities and differences between EMP and lightning. The in-flight lightning data and data taken during ground and in-flight simulated EMP testing at AFWL [41] are being used in the development of a combined EMP/natural lightning specification for the Defense Department, since this is the first data base of simulated EMP and natural lightning collected on the same aircraft with common instrumentation and test points.
- Airborne lightning location - A commercially-available airborne lightning locator system was flight tested in 1978 [6 and 7]. It was found that although such devices can provide significant additional information in the cockpit, the devices do not provide positive indications as to the location or intensity of other storm hazards, and may not provide a reliable indication of the potential for triggered lightning.
- Lightning effects on composite materials and adhesively-bonded structures - Lightning and environmental effects were studied on three composite vertical fin caps on the F-106B airplane by Howell and Fisher [42]. The three fin caps were made of fiberglass covered by a layer of flame-sprayed aluminum, Kevlar with a sacrificial outer ply of Thorstrand, and graphite/epoxy, protected by a patented graphite/epoxy lightning discharge protection rod [43] at the trailing upper apex of the unit. From visual inspection, no structural damage was detected in any of the tails. Lightning protection guidelines for adhesively-bonded composite and metal aircraft structures were developed during a corollary effect to the Storm Hazards Program [44].
- Observations of X-rays inside thunderstorms - During the Storm Hazards Program, in-situ observations of X-rays in thunderstorms were made from the F-106B airplane [45]. Significant increases in the flux of ionizing radiation inside thunderstorms were measured for the energy range 2 to greater than 12 keV and 5 to greater than 110 keV.
- Atmospheric chemistry - Levine and Shaw [46] measured enhanced levels of nitrous oxide (N_2O) associated with thunderstorm lightning. Nitrous oxide is an environmentally significant species because of its involvement in the destruction of ozone in the stratosphere and absorption and re-emission of Earth-emitted infrared radiation.
- Turbulence and windshear - Usry, et al. [14] have compared in-situ wind velocity measurements with independent wind measurements made by a ground-based Doppler radar. Although fair correlations were made between the data, it was felt that improvements in the experimental technique possibly could improve the results for such tests in the future. Independent ground-based Doppler radar studies were undertaken by the Air Force Geophysics Laboratory (AFGL) at NASA Wallops in 1981 and 1982 [28 and 29]. The relationships of turbulence, precipitation, and aircraft lightning events found during the AFGL effort have been discussed earlier in this paper. In addition, Bohne [28] found that radar methods based upon Doppler spectrum variance successfully detected regions of turbulence hazardous to aircraft.
- Airborne X-band weather radar - Although the NASA Storm Hazards Program emphasized lightning-related research, some airborne data on the performance of a commercially-available airborne X-band weather radar were collected [7 and 23]. Examples of attenuation in the X-band radar data taken aboard the F-106B airplane were noted. It was found that the judicious and intelligent use of an airborne radar (for detecting precipitation) can provide adequate information for safe avoidance of many hazardous areas. However, the airborne weather radars (and lightning locators) should be used only for avoidance of hazardous areas, not navigation through such areas.
- Lightning mishap investigations - The data and expertise gained during the Storm Hazards Program were used in support of three recent lightning mishaps within NASA during 1987. The lightning mishaps involved an airplane [47], an expendable launch vehicle [48], and three sounding rockets [49].

In summary, the NASA Storm Hazards Program has made significant contributions to the understanding of aircraft/lightning interaction and the environment associated with aircraft lightning strikes. These data can provide a strong basis for the next generation of atmospheric physics/electricity research that will follow.

4. CONCLUDING REMARKS

The experience and technical data produced by the NASA Langley Research Center Storm Hazards Program has resulted in a substantial increase in knowledge regarding lightning interactions with aircraft, and has demonstrated several ways by which the risks from lightning strikes to aircraft can be managed. These include thunderstorm avoidance, aircraft lightning protection design, and adequate maintenance. The NASA Storm Hazards Program produced the following key results in support of these goals:

1. The thunderstorm regions with highest probability for an aircraft to experience a direct lightning strike were those areas where the ambient temperature was colder than -40°C (pressure altitudes of 38 000 to 40 000 ft), where the relative turbulence and precipitation intensities were characterized as negligible to light, and where the lightning flash rate was less than 10 flashes/min. However, direct lightning strikes were encountered at nearly all temperatures and altitudes.
2. The intensity of these high-altitude lightning strikes, however, was less than that of cloud-to-earth flashes which are encountered less frequently by aircraft operating at or below the freezing level.
3. The presence and location of lightning do not necessarily coincide with the presence or location of hazardous precipitation and turbulence. In addition, hazardous precipitation and turbulence are not necessarily related to one another.

4. Airborne lightning location devices may not provide a reliable indication of the potential for triggered lightning.
5. Results of the full-scale in-flight measurements and of lightning attachment tests on a scale model have shown that initial leader attachments can occur to non-extremities such as wing leading edges, engine inlets, and the top of the fuselage, as well as to sharp extremities. These data also have shown that the entire exterior surface of this airplane may be susceptible to direct or swept lightning attachment, i.e., there are no lightning attachment Zone 3 surfaces on the F-106B airplane or on aircraft with geometries similar to that of the F-106 airplane.

5. ACKNOWLEDGMENTS

The scale-model lightning attachment tests were conducted by Messrs. J. E. Pryzby and R. J. Wood of Lightning Technologies, Inc. under NASA Contract NAS1-17703.

6. REFERENCES

1. J. A. Plumer, N. O. Rasch, and M. S. Glynn, "Recent data from the airlines lightning strike reporting project," J. Aircraft, vol. 22, pp. 429-433, 1985. (Supersedes AIAA Paper 84-2406).
2. F. A. Fisher and J. A. Plumer, "Lightning protection of aircraft," NASA Reference Publication 1008, National Aeronautics and Space Administration, Washington, DC, 1977.
3. J. C. Corbin, "Lightning interaction with USAF aircraft," Eighth International Aerospace and Ground Conference on Lightning and Static Electricity, Fort Worth, Texas, pp. 66-1 - 66-6, 1983.
4. Civil Aeronautics Board, "Aircraft accident report B-707-121, N709PA, Pan American World Airways, Inc., near Elkton, MD, Dec. 8, 1963," File No. 1-0015, Washington, DC, March 3, 1965.
5. National Transportation Safety Board, "Special investigation report-wing failure of Boeing 747-131, near Madrid, Spain, May 9, 1976," NTSB-AAR-78-12, Washington, DC, October 6, 1978.
6. B. D. Fisher and N. L. Crabill, "Summary of flight tests of an airborne lightning locator system and comparison with ground-based measurements of precipitation and turbulence," 1980 Aircraft Safety and Operating Problems, Hampton, Virginia, J. W. Stickle, Compiler, NASA CP-2170, Part 1, pp. 251-277, 1981.
7. B. D. Fisher and J. A. Plumer, "Managing risks from lightning strikes to aircraft," Flight Safety Foundation Fortieth International Air Safety Seminar, Tokyo, Japan, 1987.
8. V. Mazur, B. D. Fisher, and J. C. Gerlach, "Lightning strikes to an airplane in a thunderstorm," J. Aircraft, vol. 21, no. 8, pp. 607-611, 1984. (Supersedes AIAA Paper 84-0468.)
9. V. Mazur, B. D. Fisher, and J. C. Gerlach, "Lightning strikes to a NASA airplane penetrating thunderstorms at low altitudes," J. Aircraft, vol. 23, no. 6, pp. 499-505, 1986. (Supersedes AIAA Paper 86-0021.)
10. B. D. Fisher and J. A. Plumer, "Lightning attachment patterns and flight conditions experienced by the NASA F-106B airplane," Eighth International Aerospace and Ground Conference on Lightning and Static Electricity, Forth Worth, Texas, addendum pp. 26-1 - 26-16, 1983.
11. B. D. Fisher, P. W. Brown, and J. A. Plumer, "Research in lightning swept stroke attachment patterns and flight conditions with the NASA F-106B airplane," Tenth International Aerospace and Ground Conference on Lightning and Static Electricity, Paris, France, pp. 267-280, 1985.
12. B. D. Fisher, P. W. Brown, and J. A. Plumer, "Summary of NASA Storm Hazards lightning research, 1980-1985," International Conference on Lightning and Static Electricity, Dayton, Ohio, pp. 4-1 - 4-16, 1986.
13. B. D. Fisher, G. L. Keyser, Jr., P. L. Deal, M. E. Thomas, and F. L. Pitts," Storm Hazards '79-F-106B operations summary," NASA Technical Memorandum 81779, National Aeronautics and Space Administration, Washington, DC, 1980.
14. J. W. Usry, R. E. Dunham, Jr., and J. T. Lee, "Comparison of wind velocity in thunderstorms determined from measurements by a ground-based Doppler radar and a F-106B airplane," NASA Technical Memorandum 86348, National Aeronautics and Space Administration, Washington, DC, 1985.
15. M. E. Thomas, "Direct strike lightning measurement system," AIAA/SETP/ SFTE/SAE First Flight Testing Conference, Las Vegas, Nevada, AIAA Paper 81-2513, 1981.
16. F. L. Pitts, "Electromagnetic measurement of lightning strikes to aircraft," J. Aircraft, vol. 19, no. 3, pp. 246-250, 1982. (Supersedes AIAA Paper 81-0083.)
17. L. D. Lee, G. B. Finelli, M. E. Thomas, and F. L. Pitts, "Statistical analysis of direct-strike lightning data (1980 to 1982)," NASA Technical Paper 2252, National Aeronautics and Space Administration, Washington, DC, 1984.
18. F. L. Pitts, L. D. Lee, R. A. Perala, and T. H. Rudolph, "New methods and results for quantification of lightning-aircraft electrodynamics," NASA Technical Paper 2737, National Aeronautics and Space Administration, Washington, DC, 1987.
19. B. D. Fisher, P. W. Brown, and J. A. Plumer, "NASA Storm Hazards lightning research," Flight Safety Foundation Thirtieth Corporate Aviation Safety Seminar, Dallas/Fort Worth Airport, Texas, pp. 117-155, 1985.
20. K. P. Zaepfel, B. D. Fisher, and M. S. Ott, "Direct strike lightning photographs, swept-flash attachment patterns and flight conditions for Storm Hazards '82," NASA Technical Memorandum 87647, National Aeronautics and Space Administration, Washington, DC, 1985.
21. P. W. Brown, "Development of and results from camera systems for recording daytime lightning strikes to an airplane in flight," AIAA Twenty-fourth Aerospace Sciences Meeting, Reno, Nevada, AIAA Paper 86-0020, 1986.
22. J. C. Gerlach and R. E. Carr, "Facilities for meteorological research at the NASA Goddard/Wallops Flight Facility," Fifth Symposium on Meteorological Observations and Instrumentation, Toronto, Canada, pp. 449-453, 1983.
23. B. D. Fisher, P. W. Brown, Lt. Col. A. J. Wunschel, Jr., 1Lt. H. D. Burket, and J. S. Terry, "Joint thunderstorm operations using the NASA F-106B and FAATC/AFWAL Convair 580 airplanes," International Conference on Lightning and Static Electricity, Dayton, Ohio, pp. 20-1 - 20-10, 1986.
24. V. Mazur, J. C. Gerlach, and W. D. Rust, "Lightning flash density versus altitude and storm structure from observations with UHF- and S-band radars," Geophysical Research Letters, vol. 11, no. 1, pp. 61-64, 1984.
25. Lt. Col. K. F. Zeller, "Avoid the jolt from a bolt," in Flying Safety, pp. 2-7, February 1987.

26. D. R. Fitzgerald, "USAF flight lightning research," Lightning and Static Electricity Conference, Miami Beach, Florida, AFAL-TR-68-290, Part II, pp. 123-134, 1968. (Available from DTIC as AD 693 135.)
27. P. L. Rustan, B. P. Kuhlman, H. D. Burket, J. Reazer, and A. Serrano, "Low altitude lightning attachment to an aircraft," U.S. Air Force Technical Report AFWAL-TR-86-3009, Air Force Wright Aeronautical Laboratories, Wright-Patterson Air Force Base, Ohio, 1987.
28. A. R. Bohne, "Joint agency turbulence experiment final report," U.S. Air Force Technical Report AFGL-TR-85-0012, Air Force Geophysics Laboratory, Hanscom Air Force Base, Massachusetts, 1985.
29. A. R. Bohne and A. C. Chmela, "Storm structure during aircraft lightning strike events," J. Geophysical Research, vol. 91, pp. 13291-13298, 1986.
30. J. T. Lee and D. M. Carpenter, "1973-1977 Rough Rider turbulence-radar intensity study," FAA Report FAA-RD-78-115, Federal Aviation Administration, Washington, DC, 1979.
31. V. Mazur, B. D. Fisher, and P. W. Brown, "Cloud-to-ground strikes to the NASA F-106B airplane," AIAA Twenty-sixth Aerospace Sciences Meeting, Reno, Nevada, AIAA Paper 88-0390, 1988.
32. V. Mazur, "Lightning initiation on aircraft in thunderstorms," AIAA Twenty-sixth Aerospace Sciences Meeting, Reno, Nevada, AIAA Paper 88-0391, 1988.
33. Federal Aviation Administration, "Protection of airplane fuel systems against fuel vapor ignition due to lightning," FAA Advisory Circular AC 20-53A, Washington, DC, 1985.
34. SAE Committee AE4L, "Recommended draft advisory circular: protection of aircraft electrical/electronic systems against the indirect effects of lightning," Committee Report AE4L-87-3, Society of Automotive Engineers, Warrendale, Pennsylvania, 1987.
35. J. A. Plumer, "Further thoughts on location of lightning strike zones on aircraft," Lightning Technology, Hampton, Virginia, NASA Conference Publication 2128, FAA-RD-80-30, supplement pp. 81-98, 1980.
36. SAE Committee AE4L, "Lightning test waveforms and techniques for aerospace vehicles and hardware," Committee Report, Society of Automotive Engineers, Warrendale, Pennsylvania, 1978.
37. T. H. Rudolph, R. A. Perala, P. M. McKenna, and S. L. Parker, "Investigations into the triggered lightning response of the F-106B thunderstorm research aircraft," NASA Contractor Report 3902, National Aeronautics and Space Administration, Washington, DC, 1985.
38. R. A. Perala and T. H. Rudolph, "Triggering of lightning by aerospace vehicles," AIAA Twenty-sixth Aerospace Sciences Meeting, Reno, Nevada, AIAA Paper 88-0393, 1988.
39. J. H. Helsdon, Jr., "Atmospheric electrical modeling in support of the NASA F106 Storm Hazards Project. Final report," NASA Contractor Report 181639, National Aeronautics and Space Administration, Washington, DC, 1988.
40. V. Mazur, L. H. Ruhnke, and T. Rudolph, "Effect of E-field mill location on accuracy of electric field measurements with instrumented airplane," J. Geophysical Research, vol. 92, no. D10, pp. 12013-12019, 1987.
41. Capt. D. Andersh, 1Lt. J. Steil, K. S. H. Lee, and F. C. Yang, "Comparison of F-106B responses to natural lightning and simulated EMP," 1985 DNA/HEART Conference, Monterey, California, 1985.
42. W. E. Howell and B. D. Fisher, "In-flight environmental effects on airplane composite vertical fin caps," SAE Aerospace Technology Conference and Exposition, Long Beach, California, SAE Paper 871800, 1987.
43. C. F. Bryan, Jr., "Lightning discharge protection rod," U.S. PATENT-4,698,723, U.S. Patent Office, Washington, DC, 1987.
44. J. E. Pryzby and J. A. Plumer, "Lightning protection guidelines and test data for adhesively bonded aircraft structures," NASA Contractor Report 3762, National Aeronautics and Space Administration, Washington, DC, 1984.
45. M. McCarthy and G. K. Parks, "Further observations of X-rays inside thunderstorms," Geophysical Research Letters, vol. 12, pp. 393-396, 1985.
46. J. S. Levine and E. F. Shaw, Jr., "In situ aircraft measurements of enhanced levels of nitrous oxide associated with thunderstorm lightning," Nature, vol. 303, pp. 312-314, 1983.
47. B. D. Fisher, R. J. Taeuber, and K. E. Crouch, "Implications of a recent lightning strike to a NASA jet trainer," AIAA Twenty-sixth Aerospace Sciences Meeting, Reno, Nevada, AIAA Paper 88-0394, 1988.
48. H. J. Christian, K. Crouch, B. Fisher, V. Mazur, R. A. Perala, and L. Ruhnke," The Atlas-Centaur 67 incident," AIAA Twenty-sixth Aerospace Sciences Meeting, Reno, Nevada, AIAA Paper 88-0389, 1988.
49. W. T. Burns, Committee Chairman, "Investigation Committee final report, inadvertent launching of two test rockets and the Orion (T1-1485/30.032 UE) and the release of the restraining strap on the Taurus-Orion (T2-1422/33.052 GE) resulting from a lightning strike to launch area 2," NASA Goddard Space Flight Center/Wallops Flight Facility document, Wallops Island, Virginia, 1987.
50. B. D. Fisher, V. Mazur, J. A. Plumer, and J. C. Gerlach, "Characteristics of lightning strikes experienced by the NASA F-106B airplane," AIAA/NASA General Aviation Technology Conference, Hampton, Virginia, AIAA CP-847, pp. 37-48, 1984. (AIAA Paper 84-2237.)
51. B. D. Fisher and J. A. Plumer, "Lightning attachment patterns and flight conditions experienced by the NASA F-106B airplane from 1980 to 1983," AIAA Twenty-second Aerospace Sciences Meeting, Reno, Nevada, AIAA Paper 84-0466, 1984.

Location	Camera				Lens	
	Type	Orientation	Type	Film or Imager Size	Make/Type	Description
Aft of Cockpit	Movie	Aft-facing	Milliken DBM-54	16 mm	Century	F1.8, 5.7 mm
Cockpit	Video	Aft-facing	GE4TN2505	0.67 in.	Century	F1.8, 5.7 mm
Cockpit	Still	Aft-facing	Hassel-blad 500 EL/M	70 mm	Zeiss	Distagon, F4, 40 mm
Cockpit	Still (Stereo pair)	Forward-facing	Hassel-blad 500 EL/M	70 mm	Zeiss	Distagon, F4, 50 mm
Top of Fuselage	Video	Upward-facing	GE4TN2505	0.67 in.	Century	F1.8, 5.7 mm
Top of left wing	Video	Nose-boom-facing	GE4TN2505	0.67 in.	Century	F1.8, 5.7 mm
Top of left wing	Video	Empennage-facing	GE4TN2505	0.67 in.	Century	F1.8, 5.7 mm

Camera Location	Film/Sensor		Mode of Operation	Aperture	Neutral Density Filter	Frame rate, frame/sec (C)
	Type	Sensitivity				
Aft of Cockpit (Movie)	Kodak Ekta-chrome, MS or Video News	ASA64	Automatic (b)	F11	1.5	200
Cockpit (Video)	CID(a)	Full output at face plate. Illumination of 0.8 f.c.	Manual	F16	1.5	30
Cockpit (Still)	Vericolor II or III	ASA125 or 160	Automatic (b)	F11	None	(f)
Cockpit (Still pair)	Vericolor II or III	ASA125 or 160	Automatic (b)	F11	None	(f)
Top of fuselage (Video)	CID(a)	Full output at face plate. Illumination of 0.8 f.c.	Manual	F16	1.5	30
Top of left wing (Video pair)	CID(a)	Full output at face plate. Illumination of 0.8 f.c.	Manual	F16	1.5	30

Table 1. Characteristics of Airborne Photographic Systems Used in 1986.

Camera Location	Type	Shutter	Speed, msec
		Rotary shutter ang., deg.	
Aft of Cock-pit (Movie)	Rotary	160	2.2
Cockpit (Video)	(d)	Unshuttered. See note (d)	(d)
Cockpit (Still)	Electro-optic (e)	(e) & (f)	(f)
Cockpit (Still pair)	Electro-optic (e)	(e) & (f)	(f)
Top of fuselage (Video)	(d)	Unshuttered. See note (d)	(d)
Top of left wing (Video pair)	(d)	Unshuttered. See note (d)	(d)

Notes:
(a) General Electric Charge Induction Device (CID). Silicon 248 × 388 pixel array.
(b) Automatic mode uses 2 photographic diodes for lightning-tripped camera actuation. Sensor response is 4.5 usec.
(c) Movie camera frame rates are for steady-state operation. Acceleration/deceleration characteristics results in 126 frames in 2 sec at 200 frames/sec.
(d) 1:1 field interlace for video frame; frame integration time of 33 msec.
(e) Electro-optical between-the-lens shutter with 50 usec response time.
(f) Camera control circuitry provided the following four functions: control of shutter speed; selection and control of single and multiple-exposures-per-frame modes; and limiting of the fogging of the film frame which was in place behind the shutter, resulting from ambient light leakage through the shutter.
The single-exposure-per-frame mode allowed selecting shutter open times from 4 sec to 1/8192 sec in $(1/2)^m$ $(m = -2,-1,0,\ldots,11,12,13)$ steps. In the multiple-exposure-per-frame mode, the number of exposures could be selected in 2^n $(n = 1,2,3,\ldots,6,7,8)$ steps. There was a selectable shutter-closed time over the same range of times as the shutter-opened time control.
The film was advanced as soon as a shutter actuation cycle (up to a maximum of 256 shutter openings) was complete.
The time delay imposed by the camera control circuitry was in the nanosecond range and therefore not significant compared to other system delays.

Table 1. Concluded.

Year		1980	1981	1982	1983	1984	1985	1986	Total
Missions		19	24	35	40	38	19	9	184
Penetrations:	High	23	29	191	298	273	25	18	857
	Low	46	82	50	26	136	199	100	639
Total		69	111	241	324	409	224	118	1496
Strikes:	High	6	7	153	214	223	12	1	616
	Low	4	3	3	0	24	41	23	98
Total		10	10	156	214	247	53	24	714
Nearbys:	High	1	9	26	110	11	11	0	168
	Low	5	13	0	2	0	0	0	20
Total		6	22	26	112	11	11	0	188

Table 2. Storm Hazards Mission Summary.

Year	Month/ Day	Time, UT (hrs:min:sec)	Flight Number	Strike Number	Analysis includes:				Reference Number
					Scenario	70-mm Photos	16-mm Movie	Video	
1980	June 17	22:28:36	80-019	2	✓	(a)	(b)	(a)	10
1982	June 5	18:10:22.5	82-017	9		(a)	✓	(a)	50
1982	June 5	18:35:27.8	82-017	15	✓	(a)	✓	(a)	10
1982	June 5	18:39:46.8	82-017	16	✓	(a)	✓	(a)	10
1983	July 1	21:37:23.3	83-029	46		(a)	✓	(a)	50, 51
1983	Sept. 12	22:28:22	83-053	208	✓	(c)	✓	(a)	51
1983	Sept. 12	22:37:03.9	83-053	209		✓	(c)	(a)	51
1984	July 7	16:28:56.7	84-031	80		(a)	✓	(c)	11,19
1984	July 7	19:05:46.9	84-032	83		(a)	(c)	✓	19
1984	Aug. 9	18:59:31	84-044	197		(a)	(b)	✓	19
1984	Aug. 13	19:50:05.5	84-047	210	✓	(a)	✓	✓	9,11,19
1984	Aug. 14	19:36:51.42	84-048	214	✓	(a)	(c)	✓	9
1985	July 27	21:45:09.3	85-032	26					32(d)
1985	July 31	22:23:29.7	85-033	36					32(d)
1985	Aug. 17	19:30:33	85-037	48	✓	✓	(b)	✓	12
1986	Aug. 8	19:37:43.2	86-013	13	✓	(b)	(b)	✓	7
1986	Aug. 8	20:22:27.1	86-013	21		(c)	(c)	✓	31
1986	Aug. 8	20:23:27.3	86-013	23		✓	✓	✓	Herein

Notes: (a) Camera system not installed
(b) No data
(c) Data available; but not shown in reference
(d) Electromagnetic waveform analysis only

Table 3. Lightning strikes to the NASA F-106B airplane chosen for detailed analysis.

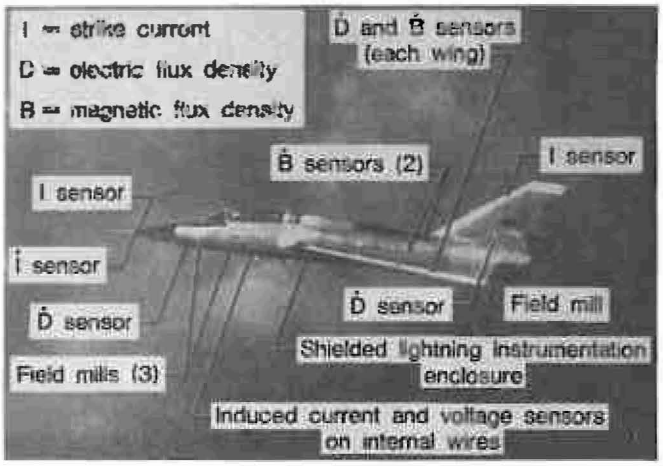

(a) Location of electromagnetic sensors.

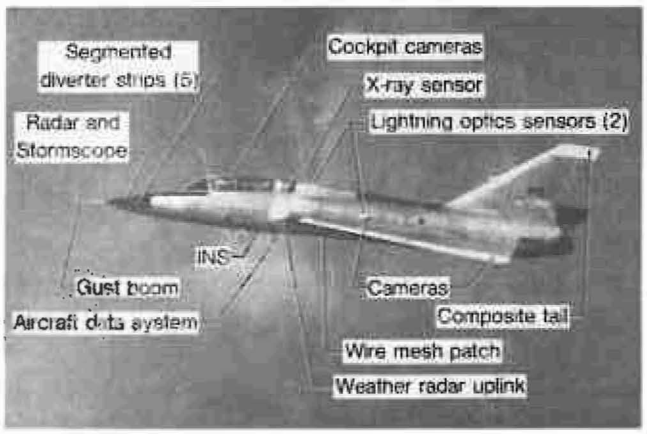

(b) Location of additional research sensors.

Fig. 1. NASA Langley Research Center F-106B Storm Hazards research airplane used from 1979-1986.

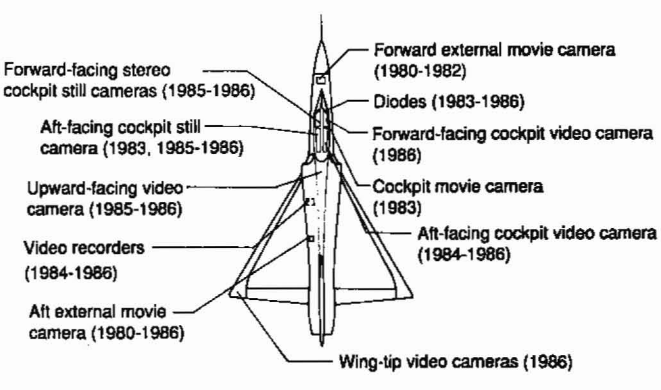

(a) Location of airborne camera systems.

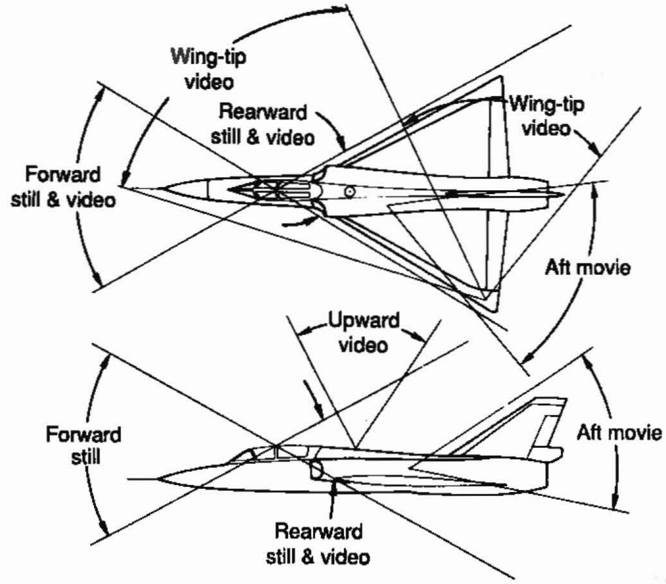

(b) Photographic and video coverage during Storm Hazards '86.

Fig. 2. Airborne camera systems used on the F-106B airplane from 1980-1986.

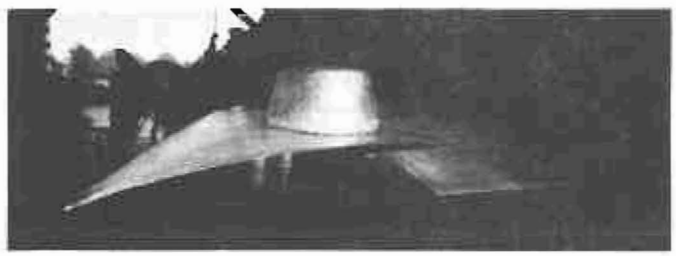

(a) View of video pod looking inboard from left wing tip. Pod has not yet been fastened to wing surface.

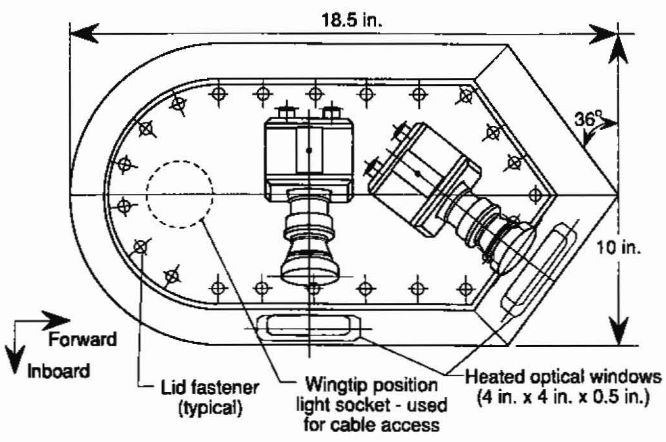

(b) Plan view of wing-tip video pod and two video cameras. Top of pod was removable for camera/wiring access.

Fig. 3. Wing-tip video pod on left wing.

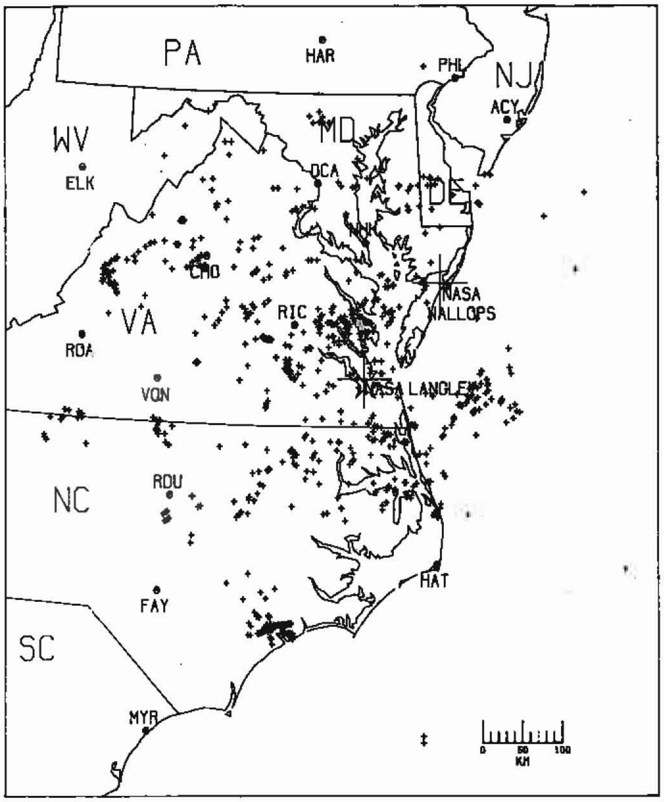

(a) Strikes. An additional three strikes occurred during flights in Oklahoma.

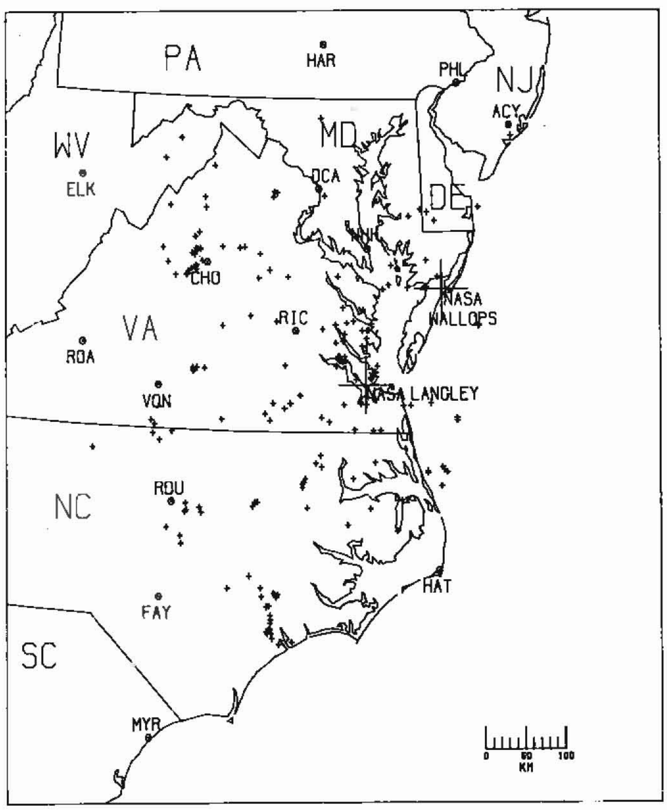

(b) Nearby flashes.

Fig. 4. Geographical locations of the F-106B airplane at times of direct strikes and nearby flashes, 1980-1986.

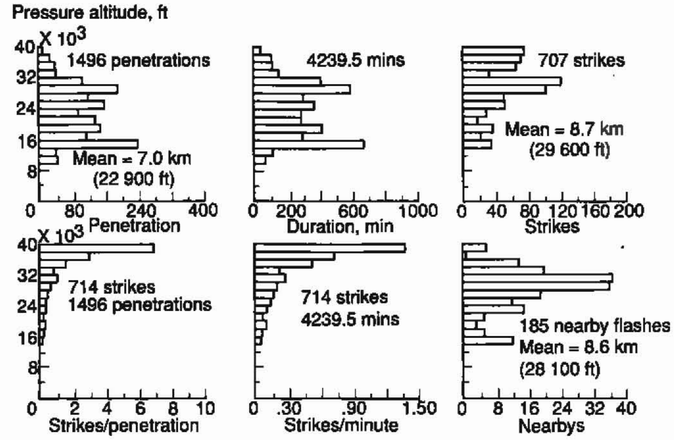

Fig. 5. Thunderstorm penetrations and lightning statistics as a function of ambient temperature for Storm Hazards '80-'86.

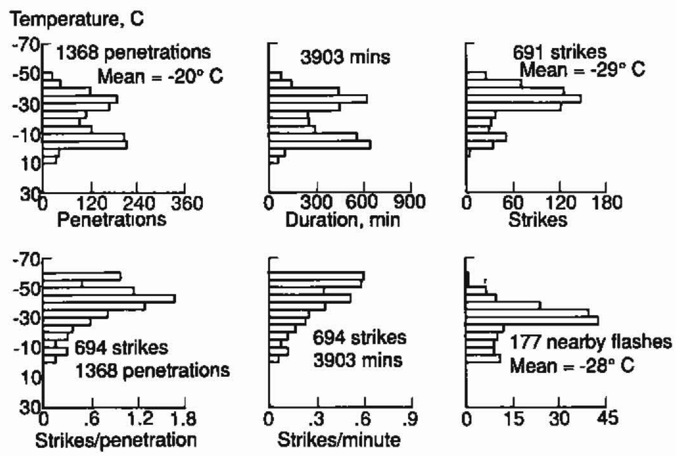

Fig. 6. Thunderstorm penetrations and lightning statistics as a function of ambient temperature for Storm Hazards '80-'86.

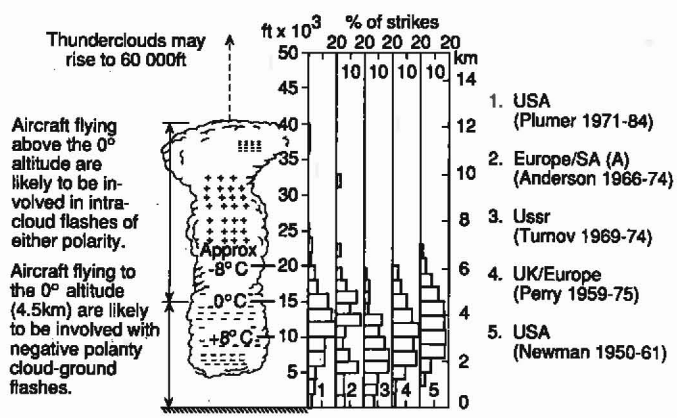

Fig. 7. Aircraft lightning strike incidents as a function of altitude. From reference 2 with updated data from reference 1.

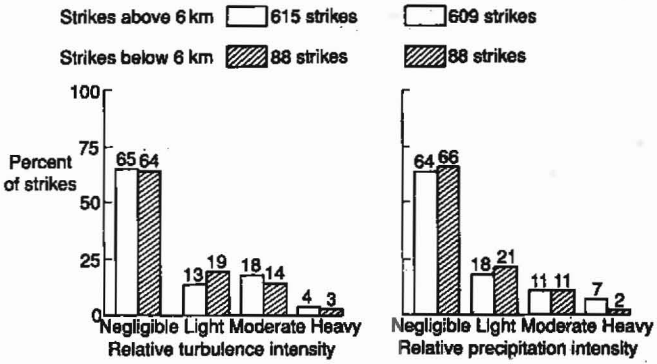

Fig. 8. Relationship of lightning strikes to relative turbulence and precipitation intensities for Storm Hazards '80-'86.

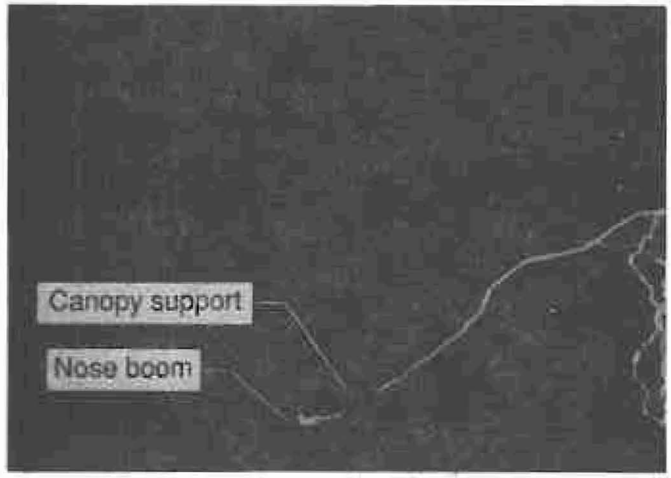

Fig. 9. Photograph of lightning strike to nose boom from 70-mm still camera on right side of cockpit. Strike 23 of 1986; 20:23:27.3 UT; Aug. 8, 1986; 15 000 ft altitude over Mathews, VA. Shutter open time of 1/512 sec; shutter closed time of 1/16 sec; f/22; 8 exposures on this frame.

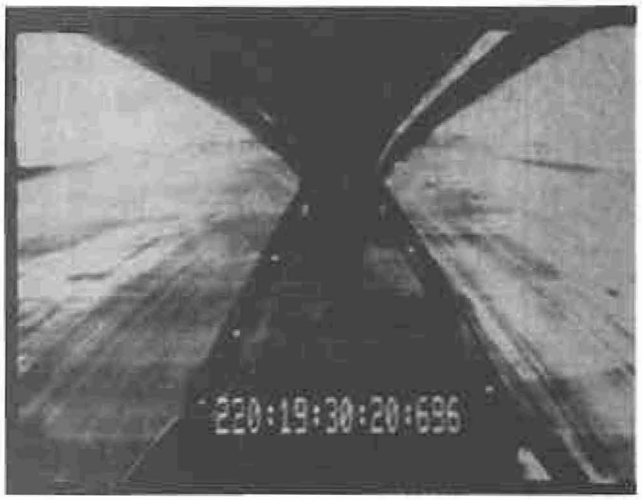

(a) Reference shot taken on the runway in sunlight.

(b) Frame 1. 20:23:27.333 UT.

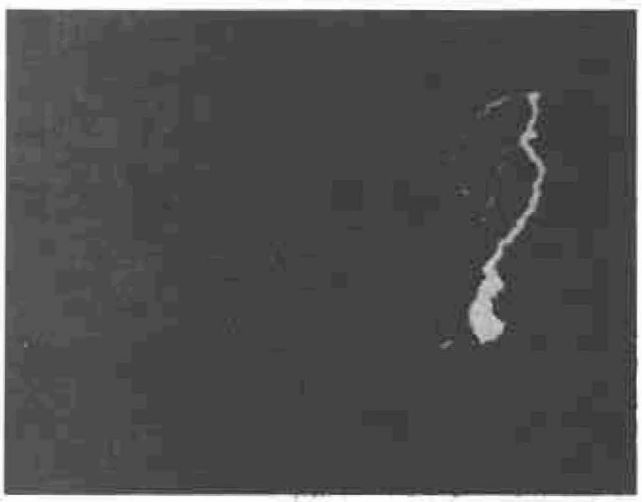

(c) Frame 2. 20:23:27.367 UT.

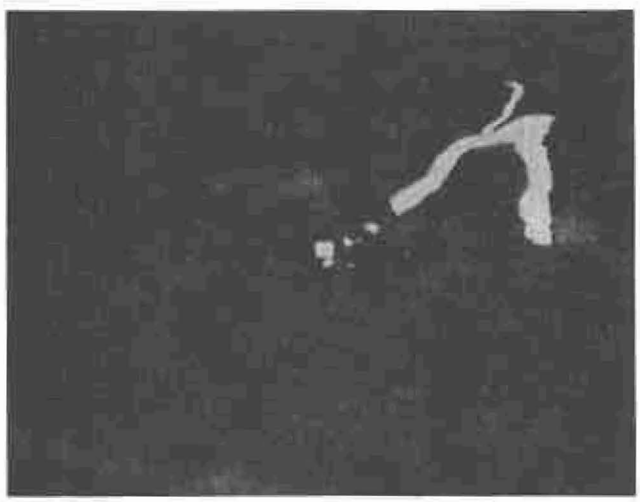

(d) Frame 3. 20:23:27.434 UT.

Fig. 10. Photographs of strike 23 of 1986 from the cockpit-mounted, forward-facing video camera.

(a) Reference shot taken on the runway in sunlight.

(b) Frame 1. 20:23:27.338 UT.

(c) Frame 2. 20:23:27.372 UT.

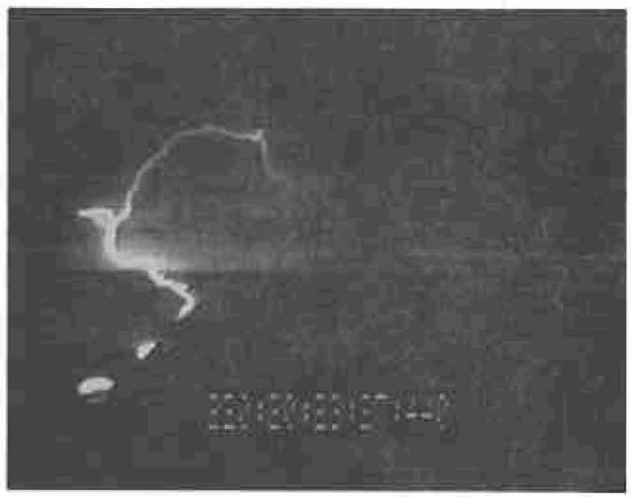

(d) Frame 3. 20:23:27.440 UT.

Fig. 11. Photographs of strike 23 of 1986 from wing-tip mounted, cockpit-facing video camera.

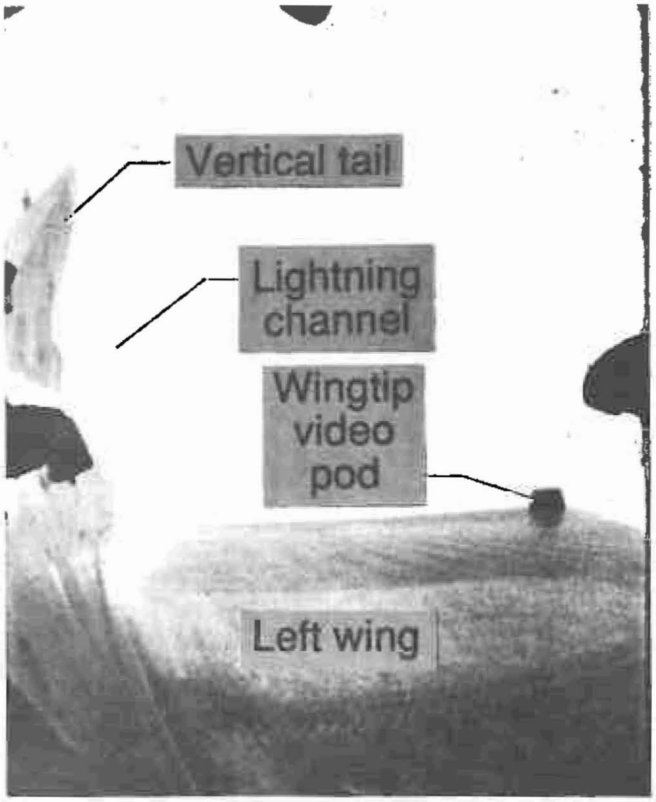

Fig. 12. Frame 3 of 167 frames from aft-facing 16-mm movie camera for strike 23 of 1986.

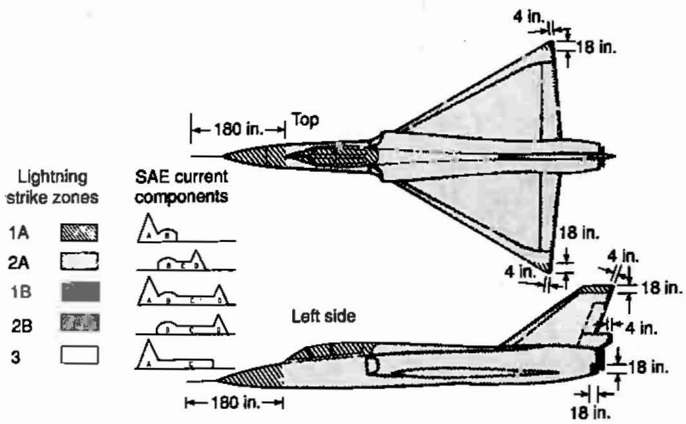

Fig. 13. Locations of lightning attachment zones on the F-106B airplane based on Storm Hazards strike data.

Fig. 14. Strike attachment to canopy with exit from nose boom of scale model. Rod electrode positioned above canopy area; positive-polarity electrode.

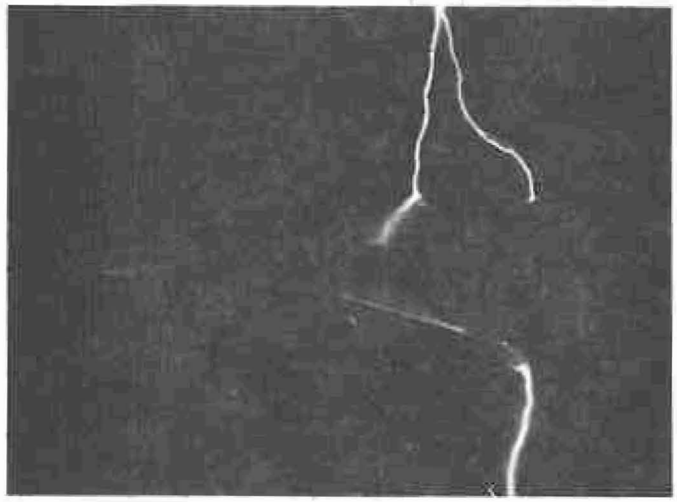

Fig. 15. Strike attachment to vertical fin and right wing tip with exit from left wing tip of scale model. Rod electrode positioned above aft fuselage area; model banked 45° left wing down; positive-polarity electrode.

Fig. 16. Strike attachments to leading edge of left wing with exit from engine exhaust area of scale model. Rod electrode positioned equidistant from nose boom and right wing tip; model pitched 45° nose up; positive polarity electrode.